4.1 RECENT PROGRESS IN THE FABRICATION AND CHARACTERIZATION OF DUCTILE-PHASE-TOUGHENED TUNGSTEN LAMINATES FOR PLASMA-FACING MATERIALS — K. H. Cunningham, G. R. Odette, K. Fields, D. Gragg, T. Yamamoto, and F. W. Zok (University of California, Santa Barbara)

OBJECTIVE

The objective of this study is to develop ductile-phase-toughened tungsten composites as candidates for plasma-facing components in future fusion reactors.

SUMMARY

A promising approach to increasing the fracture toughness of W-alloys is ductile-phase toughening (DPT). A ductile reinforcement in a brittle matrix increases toughness primarily by crack bridging. A W-Cu laminate was fabricated, and fracture resistance curves (R-curves) were calculated via precracked three-point bend testing. An analytical model of crack bridging was used to estimate the parameter space of useful toughening reinforcements for rolled W plate. Work began on extending the model framework to calculate the bridging stress-displacement function (bridging law) of a ductile reinforcement from test load-displacement data.

PROGRESS AND STATUS

Introduction

Background information and previous progress have been discussed in earlier semi-annual reports [1-4].

Experimental Procedure

Brazed W-Cu Laminate Fracture Testing

As described in the previous report, W plates were brazed with layers of Cu to form a laminate. The layup consisted of five lapped 0.85x50x50-mm W plates stacked with four alternating 75-μm Cu foils. The W plates were aligned using the rolling direction. One of the outer plates was rotated 90° from the others, as will be discussed later. Notched three-point bend bars were EDM-cut from the laminate with dimensions 21x4.65x2.125 mm, with a nominal notch depth of 0.93 mm. Specimens were separated into “edge” and “face” categories, for which the direction of crack propagation was normal to the edge or face of the ductile laminate layers, respectively. Specimens were labeled “L” or “T” with respect to the rolling direction of the W plates they contained, indicating if the crack propagation direction was parallel (L) or perpendicular (T) to the rolling direction. Specimens were also fabricated with a mixture of L and T plates, called L+T. The average W toughness and standard deviations were 13.06±2.34 and 20.90±0.45 MPa $m^{0.5}$ in the L and T directions, respectively [4].

Laminate specimens were precracked by compression-compression fatigue in the span direction as described previously for monolithic W bars [4]. Precracks were grown to an approximate target depth of a/w=0.3. Three-point bend specimens with a 20.5-mm span were tested at a crosshead displacement rate of 0.05 mm/min on an MTS load frame. A microscope mounted on the load frame was used to observe the increments of crack growth for correlation with the load-displacement data. The load (P) and displacement (D) at each increment of measured crack length (a) was used to calculate the fracture toughness corresponding to the arrested crack length following ASTM E399-12. This gives rise to a resistance [K_R(da)] curve, associated with crack bridging by the ductile layer. The crack shape at the end of each test was marked by oxidizing the W surface at 400°C in air.

Large-Scale Crack Bridging Code

The previous report discussed a large scale bridging (LSB) code we are developing with emphasis on comparing the predicted post-peak load-displacement (P-D) values to a previous model [1-7]. Our code for calculating R-curves and the pre-peak portion of load-displacement (P-D) curves was used to estimate the range of useful values for each of four parameters that describe the stress-displacement function of a ductile reinforcement ($\sigma(u)$, the bridging law) given by the flexibly parameterized Equation 1. As illustrated in Figure 1, these parameters are: the peak load (σ_{max}), the peak-load displacement (u_1), a post-peak shape exponent (n), and the failure displacement (u_2). The combination of parameters examined is shown in Table 1.

$$\sigma(u) = \frac{\sigma_{max}}{2}\left(1-\frac{u-u_1}{u_2-u_1}\right)^n + \frac{\sigma_{max}}{2}\left(1-\left(\frac{u-u_1}{u_2-u_1}\right)^{1/n}\right), u_1 < u < u_2 \qquad [1]$$

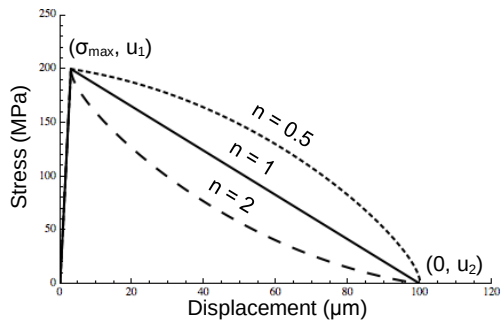

Figure 1. Example bridging stress-displacement function. The function is defined by four parameters, and assumes linear elastic behavior approaching the peak load. Examples of the effect of n on the post-peak shape are given.

Table 1. Values used for each parameter in parametric study. The resulting data set contains 256 associated R-curves and P-D curves to allow for a quantitative comparison of reinforcements for a W-matrix composite.

σ_{max} (MPa)	100	200	300	400
u_1 (μm)	1	3	5	7
n	0.3	1	3	9
u_2 (μm)	50	150	250	350

We also began work on developing an "inverse" code to estimate the ductile reinforcement $\sigma(u)$ using P-D data. The inverse code requires the same elastic constant and matrix toughness as the LSB code [4]. In principle it can extract all 4 $\sigma(u)$ parameters. However the failure displacement of the ductile reinforcements, u_2, usually can be obtained from measurements on the broken specimens, hence this was fixed in this exercise. The basic algorithm is as follows:

- Store the R-curve data points as an interpolated function.
- Estimate the elastic portion of the bridging law:
  - Guess low values for σ_{max} and u_1 (1 MPa and 0.1 μm).
  - Model a very short crack extension to ensure that the opening displacement is less than u_1.
  - Run the LSB model to calculate the crack shape u(x), crack-face stress distribution σ(x), and K_R using the interpolation function.
  - Calculate the ratio of the measured increase in fracture resistance to the calculated increase in fracture resistance, $(K_{R,test} - K_I)/(K_{R,calc} - K_I)$, where K_I is the known toughness of the matrix.
  - Multiply σ_{max} by the K ratio to update the estimated value, and iterate until σ_{max} converges.
  - Save the (σ_{max}, u_1) point, then increase the u_1 guess by a small amount and repeat.

- End the iterative process when the convergent σ_{max} value begins to decrease between iterations.
- Estimate the post-peak shape:
  - Guess a value for n (1 is simplest).
  - Model $K_R(da)$ using the first measured K_R point after crack initiation in the test data.
  - Follow the same procedure as above, except dividing n by the K ratio with each iteration.
  - Manually choose an appropriate n value based on the resulting plot of n versus a.

Results

Brazed W-Cu Laminate Fracture Testing

No face-orientation composite was tested because the compression-compression precracking method caused shear failure at the W-Cu interfaces. Edge-orientation fracture was characterized by varying increments of unstable crack growth followed by crack arrest (pop-ins) due to the Cu reinforcement, as illustrated in Figure 2 from an L+T oriented specimen. A representative fracture surface image of a heat-tinted sample is shown in Figure 3 from the same L+T specimen. Precrack fronts had a concave or flat shape instead of the usual convex "thumbnail" shape, and in the mixed orientation the crack propagated to a greater depth in the L-oriented versus T-oriented plates. This is qualitatively consistent with the anisotropic toughness of the W matrix, as the rolled plate is tougher in the T direction than the L direction by a factor of about 1.6 [4].

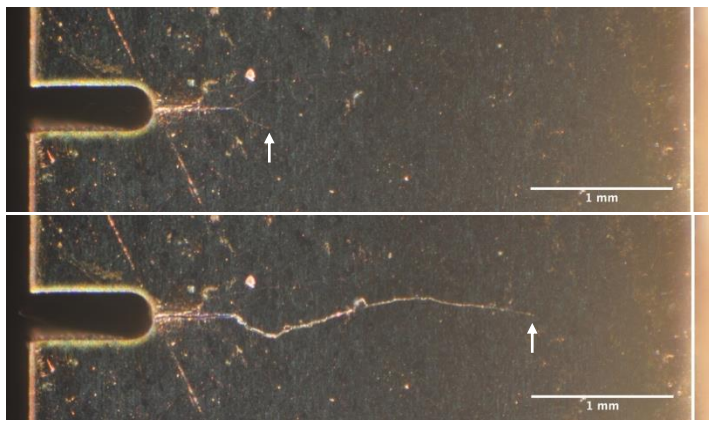

Figure 2. Comparison of two successive images from three-point bend testing on W-Cu laminate (specimen O3-2). The crack at a/w=0.36 (top) grows unstably to a/w=0.76 (bottom) before being arrested by the Cu reinforcement. Arrows indicate the crack tip in each image, and the vertical line at right indicates the edge of the specimen.

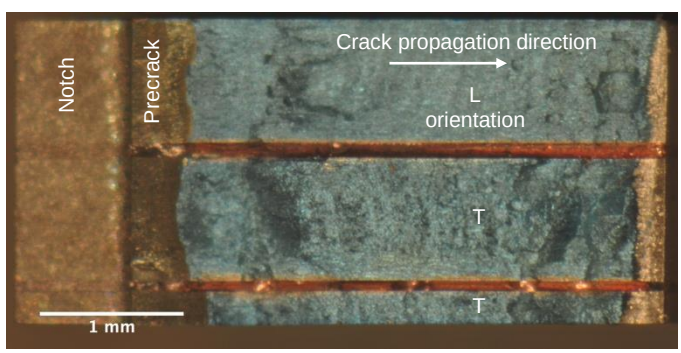

Figure 3. Fracture surface of W-Cu laminate bend bar (O3-2). Blue coloration on W layers is from heat tinting to observe the final crack length in different W plates. Crack is longer in L-oriented plate than in T

plates. Dark contrast in blue test crack region is from surface features; L plate has relatively flat fracture surface while T plates are rough.

A representative P-D curve along with the corresponding R-curve is shown in Figure 4, illustrating the load drops associated with unstable crack growth as well as the loads used to calculate each point in the R-curve. A summary of all calculated R-curves is given in Figure 5 as a set of plots grouping tests by orientation (L, T, or L+T). The T orientation showed greater increases in toughness with crack extension than the L orientation, but had less stable crack growth. For the mixed orientation, in which one of the three W plates was a different orientation than the other two (one L and two T, or vice versa), had a small initial increment of higher R-curve slope than the L orientation, but plateaued around a/w=0.5, and reached a maximum K_R between those for the L and T orientations at very large a/w. Again, this behavior simply reflects the differences in the T and L matrix toughness. These data do not show a significant difference in R-curve behavior between areas of the laminate containing 2L+1T versus 1L+2T plates.

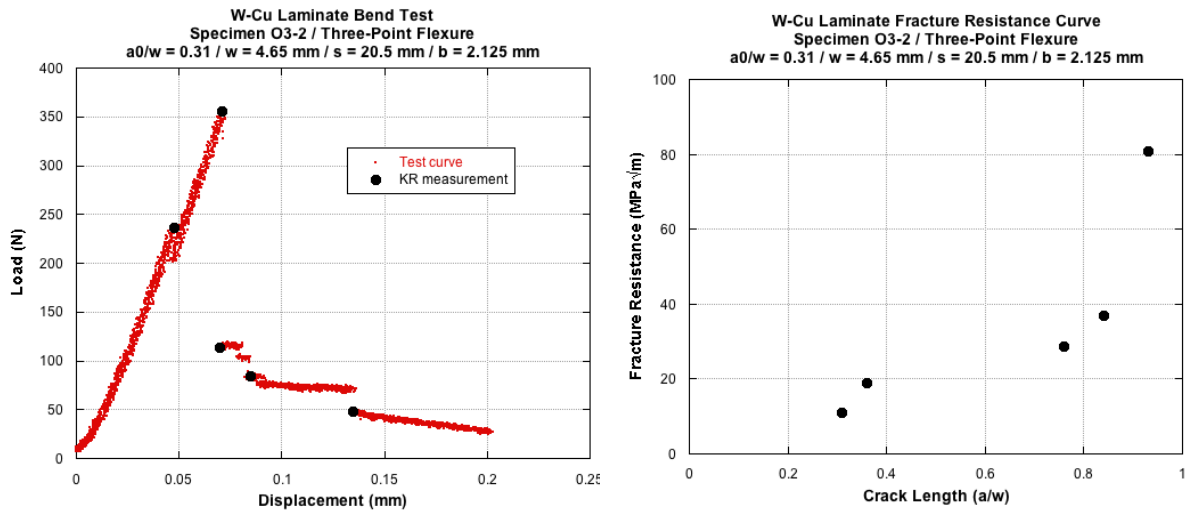

Figure 4. P-D curve (left) and R-curve (right) for W-Cu laminate bend specimen O3-2. Black points on P-D curve indicate the maximum load at each measured crack length used to calculate K_R. Significant load drops were observed corresponding to unstable crack growth and subsequent crack arrest.

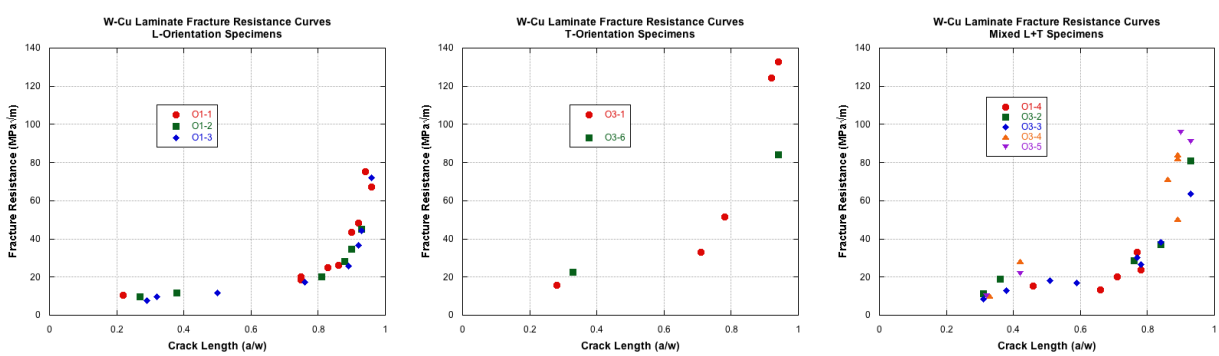

Figure 5. Comparison of R-curves for W-Cu laminate in different orientations. Plots are grouped by laminate orientation: specimens with only L-orientation W plates (left), only T-orientation plates (center), or a mix of L and T plates (right). The T orientation has higher initiation toughness as expected, as well as a greater increase in fracture resistance with crack growth. The L orientation shows more stable crack growth, evidenced by the greater number of points per test. In the mixed orientation, initiation toughness appears controlled by the L orientation, with the subsequent R-curve shape a mixed character of L and T.

Since the K_R curves show significant toughness increases only at large a/w, one might conclude that the small amount (< 8% by volume) of relatively weak (annealed Cu) and thin reinforcement had little beneficial effects on the fracture resistance of the composite versus the monolithic W. Indeed this is the case if the metric is the relative engineering strength of the composite. However, crack arrest and increments of quasi-stable growth are observed, providing some degree of engineering ductility in the composite that is entirely absent in the monolithic W plate. Therefore, a composite with a higher volume fraction of stronger reinforcing phase, with an optimized thickness, would be expected to perform significantly better. To this end, we used our crack bridging model to guide the fabrication of an improved composite.

Large-Scale Crack Bridging Code

A parametric study of reinforcement $\sigma(u)$ was used to evaluate the effects of the controlling parameters individually and in combination as illustrated in Figure 6. Here the P-D curves are normalized by the corresponding loads and displacements at elastic fracture of the brittle matrix, P' and D', respectively.

σ_{max} (MPa)	u_1 (μm)	n	u_2 (μm)	P-D Curves [P/P' vs. D/D']	R-Curves [K_R (MPa) vs. a/w]
100 200 300 400	1	0.3	350	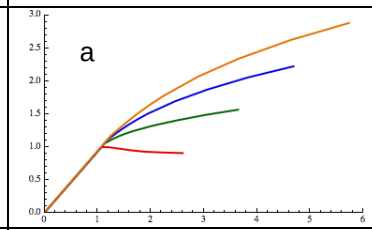	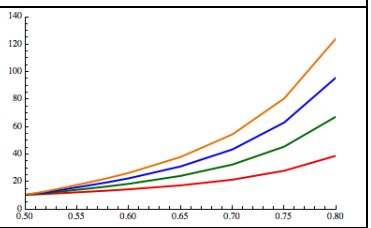
400	1 3 5 7	0.3	350	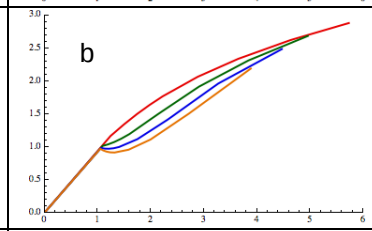	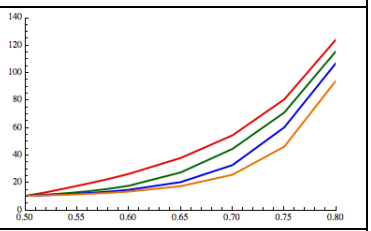
400	1	0.3 1 3 9	350	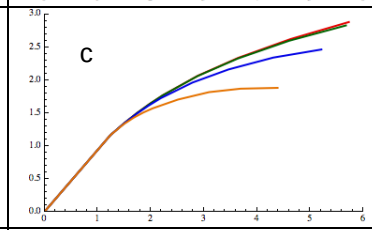	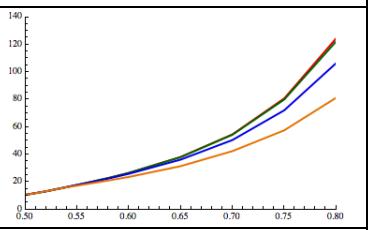
400	1	9	50 150 250 350	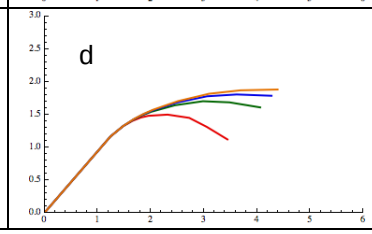	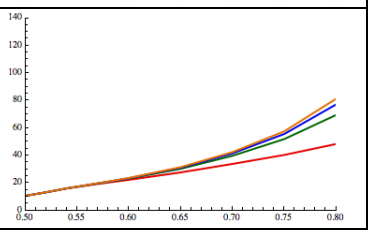

Figure 6. Parametric study summary. In each row of values and plots, one parameter is varied and the resulting P-D curves and R-curves are shown. Load and displacement values are normalized by the load capacity (P') and displacement (D') at fracture, respectively, of the unreinforced tungsten matrix. The mechanical behavior of the composite is more sensitive to σ_{max} and u_1 than to n and u_2**.**

For a desirable, and expected, low value of u_1, the P-D and K_R(da/w) curves increase with increasing σ_{max}, resulting in a desirable increase in P_{max}, accompanied by increasing D or ductility (Figure 6a). The

detrimental effect of increasing u_1 is also revealed in the P-D curves (Figure 6b). Both increasing the convex shape of the bridging law (Figure 6c) and, to a lesser extent, increasing u_2 (Figure 6d) increase the composite strength and ductility P-D curves.

It must be emphasized that while these effects can be qualitatively anticipated, they all represent LSB effects for a growing bridging zone that cannot be quantitatively predicted based on "intuition" or simple energy-based concepts. Such mistaken and misleading thinking is unfortunately all too common. The engineering performance capabilities of a DPT composite are reflected in the normalized P-D curves with values of P/P' and D/D' greater than 1, which is the limit for the elastically brittle monolithic matrix material. It is also worth noting that it is the initial slope of the $K_R(da)$ curve that controls the crack growth initiation P-D and any subsequent stable crack growth for any expected practical initial crack length.

It is generally not possible to directly measure $\sigma(u)$ curves for embedded reinforcements since this depends on details like debonding and triaxial stresses in matrix cracks that are blunted in the ductile phase. However, as noted above they can be inversely extracted from P-D data [6,7]. The estimation strategy for σ_{max} and u_1 successfully reconstructed the elastic loading portion of the bridging law in cases where the true u_1 value was 5 μm or less. Assuming that u_2 is a measurable quantity, the estimate for n also converges to the correct value for intermediate values of a/w as illustrated in Figure 7. The estimation algorithm described can be used to estimate a relatively narrow range of $\sigma(u)$ parameters, but this is still work in progress.

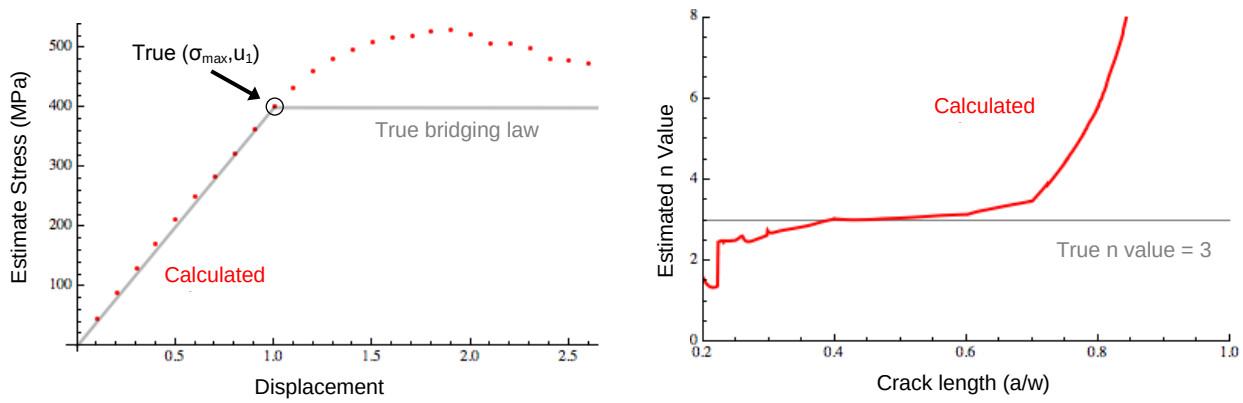

Figure 7. Summary of bridging law estimation from simulated test data. Left: estimate of (σ_{max},u_1) point shown against a close-up view of the true bridging law. Calculated values track well with the true elastic slope of the bridging law. Without knowing the true bridging law that was used to construct the R-curve that the estimate uses, it is difficult to determine the true point, even though it has been estimated quite accurately. Right: estimate of n parameter shown as the values calculated at a variety of crack lengths. The plateau around a/w=0.45 is the correct estimate of the true n value, but as with (σ_{max},u_1) it is difficult to choose an exact value from the estimates alone.

Ongoing and Future Work

The large-scale bridging model will be finalized with respect to the calculation of P-D and $K_R(da)$ curves for a given $\sigma(u)$, and the "inverse" calculation of $\sigma(u)$ from given P-D data.

References

[1] K. H. Cunningham, K. Fields, D. Gragg, F. W. Zok, C. H. Henager, Jr, R. J. Kurtz, and T. Roosendaal, Recent Progress in the Development of Ductile-Phase Toughened Tungsten for Plasma-Facing Materials, in DOE/ER-0313/54 - Volume 54, Semiannual Progress Report, June 30, 2013. 2013, US DOE: ORNL, TN.

[2] C. H. Henager, Jr, R. J. Kurtz, T. J. Roosendaal, B. A. Borlaug, G. R. Odette, K. H. Cunningham, K. Fields, D. Gragg, and F. W. Zok, Recent Progress in the Development of Ductile-Phase Toughened Tungsten for Plasma-Facing Materials, in DOE/ER-0313/55 - Volume 55, Semiannual Progress Report, Dec. 31, 2013. 2013, US DOE: ORNL, TN.
[3] K. H. Cunningham, G. R. Odette, K. Fields, D. Gragg, F. W. Zok, C. H. Henager, Jr., R. J. Kurtz, T. J. Roosendaal, and B. A. Borlaug, Recent Progress in the Fabrication and Characterization of Ductile-Phase-Toughened Tungsten Composites For Plasma-Facing Materials, in DOE/ER-0313/56 - Volume 56, Semiannual Progress Report, Jun. 30, 2014. 2014, US DOE: ORNL, TN.
[4] K. H. Cunningham, G. R. Odette, K. Fields, D. Gragg, T. Yamamoto, F. W. Zok, C. H. Henager, Jr., R. J. Kurtz, T. J. Roosendaal, and B. A. Borlaug, Recent Progress in the Fabrication and Characterization of Ductile-Phase-Toughened Tungsten Laminates For Plasma-Facing Materials, in DOE/ER-0313/57 - Volume 57, Semiannual Progress Report, Dec. 31, 2014. 2014, US DOE: ORNL, TN.
[5] G. R. Odette, B. L. Chao, J. W. Sheckherd, and G. E. Lucas. Acta Metall. Mater. 40-9 (1992) 2381-2389.
[6] G. R. Odette and B. L. Chao, unpublished notes.
[7] J. A. Heathcote. Ph.D. Dissertation, University of California, Santa Barbara, 1996.